

El Niño and Indian summer monsoon rainfall relationship in retrospective seasonal prediction runs: experiments with coupled global climate models and MMEs

P. K. Pradhan¹ · Venkatraman Prasanna² · Doo Young Lee³ · Myong-In Lee⁴

Received: 29 September 2014 / Accepted: 29 July 2015 / Published online: 28 August 2015
© Springer-Verlag Wien 2015

Abstract The relationship between the warm phase of El Niño southern oscillation (ENSO) and Indian summer monsoon rainfall is explored through seven coupled global climate models (CGCMs), which are semi-operational at APEC Climate Center (APCC). The 23-year (1983–2005) hindcast datasets of individual model ensembles derived from May initial conditions for southwest monsoon season (JJAS) are utilized to find out the simultaneous influence of El Niño–ISMR relationship in 1990s, which is observed to be weaker than present decades. The hindcast of ISMR climatology derived from seven individual models viz. APCC, NCEP, POAMA, SINT, SUT1, PNU and UHT1 appears to be reasonably simulated; in particular, about 50 % of mean departure is evident in most CGCMs. In addition, four of six El Niño years during the aforementioned period are well depicted in most of the CGCMs, while the years 1994 and 1997 are not represented well by these seven individual models. The warm SST anomaly aligned with surplus precipitation over tropical equatorial Pacific region simulated using APCC, NCEP, POAMA, SINT and SUT1 is relatively better than that simulated in

PNU and UHT1 and it is closer to observation. The El Niño–ISMR teleconnection skills both monthly to seasonal scale are very poor in PNU as well as UHT1 and their RMSEs are 3.84 and 3.77 higher than APCC, NCEP, POAMA, SINT and SUT1 models. The authors developed two Multi-Model Ensembles (MMEs) that were simple composites of ensemble forecast from seven models (APCC, NCEP, POAMA, SINT, SUT1, PNU and UHT1) referred to as MME1, and from five models (APCC, NCEP, POAMA, SINT and SUT1) are referred to as MME2. Importantly, the one-month lead MME2 prediction of anomaly correlation coefficient (ACC) and its adverse impacts is reasonably better than MME1 prediction. However, there are some limitations in capturing SST forcing fields over Indian Ocean region in both MMEs. Among the seven models, SINT has the highest pattern correlation of precipitation over the Indian monsoon region.

1 Introduction

The Asian monsoon climate is significantly dominated by Indian summer monsoon rainfall (ISMR). Every year, more than 80 % of annual rainfall is received over only the Indian land grid points, the so-called all-India summer monsoon rainfall index (hereafter AISMR), as reported by Parthasarathy et al. (1994). During a short period of 4 months from June through September (JJAS), the AISMR significantly affects agriculture, economy and living status of the people of Indian subcontinent. It appears to have year-to-year fluctuations, and the most prominent variation on the interannual scale is between the so-called good (poor) with above-average (deficient) rainfall strongly related with food

Responsible Editor: M. Kaplan.

✉ P. K. Pradhan
prabodhakumar@gmail.com

¹ University of Tras-os-Montes e Alto Douro,
5001801 Vila Real, Portugal

² APEC Climate Center (APCC), Busan 612 020,
Republic of Korea

³ Department of Atmospheric Sciences, Pusan National
University, Busan 609735, Republic of Korea

⁴ Ulsan National Institute of Science and Technology,
Ulsan 689 798, Republic of Korea

productivity, while the modest decrease of 10 % of long-term mean rainfall leads to significant decrease in rice production in India (Swaminathan 1987; Abrol and Gadgil 1999). In addition, the interannual variability of AISMR is expected to have a larger impact on yield of agricultural products of the country in the coming years (Gadgil 1995; Webster et al. 1998). Therefore, the prediction of AISMR is very essential for agricultural sectors. It has been understood that deficient/surplus AISMR is related to the individual influences of warm/cooling phases of El Niño Southern Oscillation (ENSO) in seasonal to interannual scales (Sikka 1980; Mooley and Parthasarathy 1984a, b; Kripalani and Kulkarni 1999; Kumar et al. 1999; Ailikon and Yasunari 2001). Since the works by Walker (1923), numerous studies have documented the teleconnection between interannual variability of ISMR with ENSO since the past 180 years. Therefore, this relationship has been analyzed and discussed (Charney and Shukla 1981; Rasmusson and Carpenter 1983; Barnett 1984; Kumar et al. 1995; Webster et al. 1998; Slingo 1999; Annamalai et al. 1999; Behera et al. 1999; Slingo and Annamalai 2000; Krishnamurthy and Goswami 2000; Kirtman and Shukla 2000; Goswami and Jayavelu 2001; Krishnan et al. 2000; Gadgil et al. 2004). A critical analysis by Kripalani and Kulkarni (1999) documented the droughts in India which are caused by El Niño forcing much more severe than non-El Niño episodes. Thus, ISM response to El Niño has been given more importance since several decades.

Recent findings by Rajeevan and Pai (2006) suggested that the SST anomaly (SSTA) over the Niño 3.4 region (Trenberth 1997) in the central Pacific region might be a better indicator for the association than the combined index derived from Niño 3 and Trans Niño Index (TNI). Therefore, the reliable exhaustive long records of AISMR were considered using the Indian Institute of Tropical Meteorology (IITM) rainfall datasets with Niño 3.4 index. The details of these rainfall datasets are discussed in (Parthasarathy et al. 1994). The Index can be obtained from the website <http://www.tropmet.res.in>. The normalized AISMR and Niño 3.4 index during 150 years from 1861 to 2011 observations are analyzed in terms of 30-year interval and listed in Table 1. The correlation coefficients (CC) between the Pacific SST over the Niño 3.4 region with AISMR are found to be -0.15 , -0.67 , -0.71 , -0.62 and -0.47 , respectively, for subsequent intervals (Table 1). However, the CC between the Pacific SST with AISMR in the recent decades shows weak relationships as compared to 30 years ago. Only recent three decades, from 1980 to 2011 have been considered in this study. While model hindcast datasets are available at APCC for 1983–2005, ENSO–monsoon relationships compared with observation for the same period are as shown in Fig. 1. The results show that (as highlighted by vertical black and spotted

Table 1 The 150-year correlation coefficients (CC) between the SST anomalies over Niño 3.4 region (predictor) with all-India summer monsoon rainfall (AISMR) anomalies during the JJAS period of 1861–2011

Time period	CC AISMR with SST anomaly over the tropical Pacific Ocean Niño 3.4 index
1861–2011	-0.52
1861–1890	-0.15
1891–1920	-0.67
1921–1950	-0.71
1951–1980	-0.62
1981–2011	-0.47
1983–2005	-0.48

bars) most of deficient (excess) monsoon have been associated with El Niño (La Niña) events.

The teleconnection characteristic between AISMR with Niño 3.4 index became noticeably weaker during 1983–2005 [cc: -0.48] (approximately 15 %) than those of the past three decades (1950–1980). This weakening relationship has also been documented in several papers (Kumar et al. 1999, 2006; Gershunov et al. 2001; Ashok et al. 2001, 2004; Kinter et al. 2002; Annamalai et al. 2007; Kucharski et al. 2007, 2008; Xavier et al. 2007; Boschat et al. 2012). This is an important question since the ability to forecast ENSO up to 1 year in advance has shown increasing skill in recent years (e.g., Latif et al. 1998). If the monsoon–ENSO relationship remains reasonably constant rather than weakening in the future, then interannual fluctuations of the monsoon may have some hope in predictions. Otherwise, if this relationship fails, then the prominent indicator of year-to-year monsoon variability remains precarious (Annamalai et al. 2007). However, it would be difficult to produce monsoon epochs in interannual time scales. The prime objective of this paper is to determine the fidelity of individual CGCMs on prediction of AISMR in weak and strong ENSO conditions in the recent decades.

The ISMR prediction skills through statistical (Rajeevan et al. 2004, 2007) and atmospheric global model (AGCM) are discussed (see Gadgil and Sajani 1998; Kang et al. 2002; Wang et al. 2004; Rajeevan and Nanjundiah 2009). The recent study by Gadgil et al. (2005) addresses the insufficiency of these models, even though the India Meteorological Department (IMD) current operational statistical model could not predict the major drought conditions such as those of 2002, 2004, and 2009. It is expected that the reliable seasonal prediction of ISMR is possible only through coupled global climate model (CGCM) instead of AGCM and statistical models. However, the prediction skills over the tropical Indo-Pacific

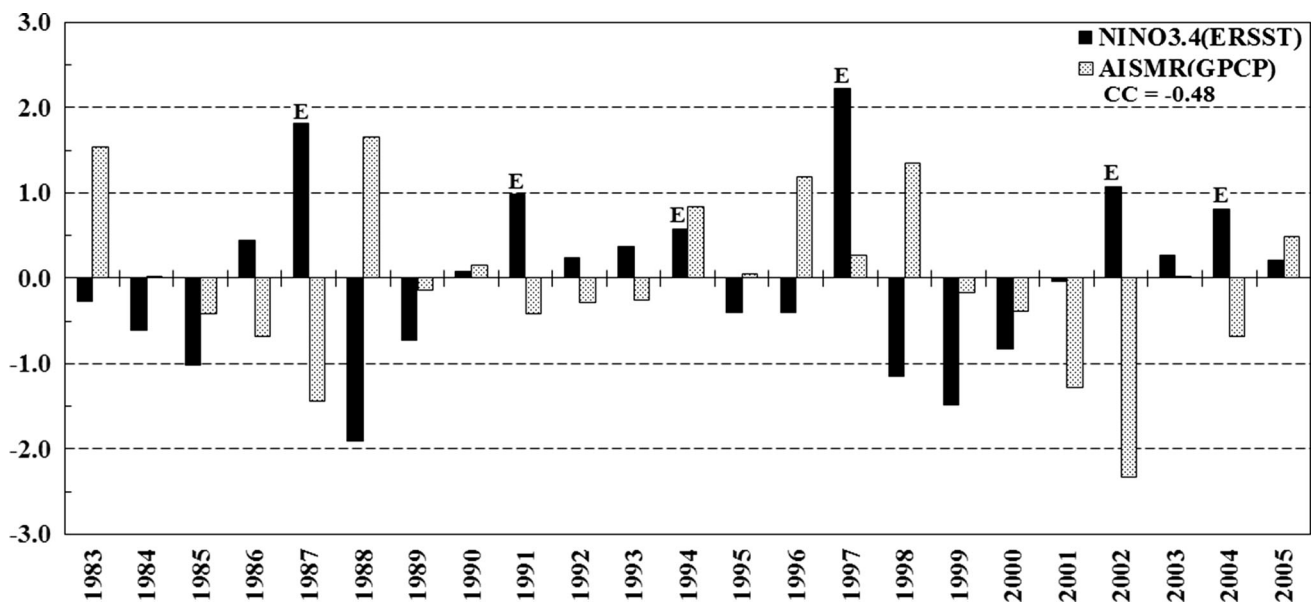


Fig. 1 Year-year variability of normalized all-Indian summer monsoon rainfall anomaly (AISMR) and Niño 3.4 index (*black shaded*) anomaly for the period of 1983–2005

regimes such as ENSO, Indian Ocean Dipole (IOD) mode (Saji et al. 1999) and the Equatorial Indian Ocean Oscillation (EQUINOO), (Janakiraman et al. 2011; Gadgil and Srinivasan 2011) are significantly better in CGCMs rather than AGCMs. Thus, CGCMs have become reliable tool for dynamical seasonal prediction. Currently, most of the operational climate prediction centers provide real-time forecast 3–6 months in advance (Barnston et al. 2012). Though the dynamical models have made significant improvements in model physics and dynamics in last few years, the present-day AGCMs could not simulate the mean and interannual variability of Indian summer monsoon successfully (Kang et al. 2002). It is also found that the skill of the AGCM is poorer in simulating Indian monsoon due to lack of proper representation of realistic sea surface temperature (Shukla et al. 1996). The forecast errors in the seasonal prediction can be reduced through the combinations of the ensemble member's forecast (Branković et al. 1990; Brankovic and Palmer 2000). Therefore, many studies now mainly focus on multi-model ensemble and super ensemble forecast techniques (see Krishnamurti et al. 1999; Wu and Kirtman 2003; Wang et al. 2004; Chakraborty and Krishnamurti 2006; Rajeevan et al. 2012; Acharya et al. 2011a, b) for the seasonal and interannual prediction of monsoon.

One approach is to generate the multi-model ensembles (MMEs) forecast based on combination of individual model with perturbed initial conditions (Lorenz 1969), which would provide better prediction of ISMR. However, the skill of MME depends on the fidelity of individual

models; thus, the evaluation of CGCMs is very essential. The prediction skills of seven CGCMs are discussed here and the study is divided into five sections. The observational and CGCMs datasets are introduced in Sect. 2. In Sect. 3, the mean monsoon rainfall climatology and their biases are investigated. In addition, the anomalous features of El Niño composites are also discussed in Sect. 3. The skill of AISMR and ENSO teleconnection is discussed in Sect. 4. During the weak ENSO conditions, the performance of the MMEs and prediction of AISMR by the individual CGCMs are discussed in Sect. 5 and discussion and conclusions are provided in Sect. 6.

2 Data and methodology

The hindcast datasets are derived from seven fully coupled global climate models (CGCMs) for 1-month lead MMEs forecast using May initial conditions has been semi-operational since 2009 at Asian Pacific Economic Cooperation (APEC) Climate Center, Busan, and they are used in the present study. The details of the aforementioned models are given in Table 2. These CGCMs viz. APCC, NCEP, PNU, POAMA, SINT, SUT1, and UHT1 outputs have been obtained through Climate Prediction (CliPAS) project, which has been planned for climate prediction (Wang et al. 2009; Ham and Kang 2011; Lee et al. 2010) of APEC region. Information regarding these models and the respective initial conditions has been discussed by Wang et al. (2009) and Jeong et al. (2012, 2008).

Table 2 Combination of ocean and atmospheric models used for coupled GCMs at APCC/CliPASProgramme

Sl. no	Name of the model	Host organization	AGCM horizontal/vertical resolution	OGCM horizontal/vertical resolution	Ensemble member	Forecast period	References
1	CCSM3	APCC	CAM3T85 L26	POP1.3 gxlv3 L40	5	1983–2008	Jeong et al. (2008)
2	CFS	NCEP	GFS T62/L64	MOM2.2 1/3 Lat x 1lon L40	15	1981–2006	Saha et al. (2006)
3	PNU	PNU	CCM3 T42L18	MOM3 ~ 0.7 (low lat) ~ 1.4 (mid lat) and ~ 2.8 (high lat) L29	10	1979–2008	Sun and Ahn (2011)
4	POAMA	BOM	BAM 3.0d T47/L17	ACOM2 0.5–1.5lat x 2lon L31	10	1981–2006	Zhao and Hendon (2009)
5	SINT	FRCGC	ECHAM4 T106/L19	OPA 8.2 2 cos (lat) x 2 lon L31	9	1981–2009	Luo et al. (2005)
6	SUT1	SNU	SNU T42/L21	MOM2.2 1/3lat x 1lon L32	6	1981–2009	Ham and Kang (2011)
7	UHT1	UH	ECHAM4 T31/L19	UH Ocean 1latx2lon L2	10	1982–2005	Fu and Wang (2004)

The extended reconstructed monthly sea surface temperature (ERSSTV3, which includes satellite data) from National Ocean Atmosphere Administration (NOAA) ($2^\circ \times 2^\circ$) resolution available at <http://www.ncdc.noaa.gov/ersst> (Smith et al. 2005), the gridded precipitation data from the Global Precipitation Climatology Project version 2 (GPCP v2) ($2.5^\circ \times 2.5^\circ$) (Adler et al. 2003) resolution are used. These datasets have been linearly interpolated as per the model resolution in concern. Atmospheric variables such as wind fields are obtained from National Center for Environmental Prediction, Department of Energy (NCEP/DOE-II) reanalysis data (Kanamitsu et al. 2002a, b). We have examined the composite precipitation and SST anomaly over the Asian monsoon region from MMEs and compared with the observation. The AISMR anomaly calculated from the monthly mean sub-divisional rainfall dataset available from IITM for the period of 1831–2011 is used in this study. To explore the 150 years of teleconnection characteristics with ENSO–monsoon relationship, the correlation coefficients among the AISMR and Niño 3.4 SST anomaly (area average of 5°S – 5°N ; 170°E – 60°W) from ERSST V3 have been evaluated.

To examine the CGCMs fidelity, 1-month lead seasonal prediction for JJAS period of 1983–2005 climatology and bias has been calculated. To identify the dominant features during this aforementioned period, the seasonal anomaly was calculated. However, in each model, the ensemble mean anomalies are calculated based on the monthly ensemble member mean climatology for each lead-time. Some additional calculations such as composites analysis, temporal and spatial correlation coefficients have been employed to investigate the relationship between observation and individual CGCMs. Using the best models among the seven CGCMs, the MME forecast for AISMR–ENSO relationship is also discussed.

3 Hindcast skills for predicting relation between El Niño and Indian summer monsoon

3.1 Climatology and bias

To understand the prediction skill of the individual CGCMs, mean ensemble products available in APCC and the precipitation over the ISM region during JJAS are investigated on the basis of climatology, bias, and their map-to-map correlation coefficients (CC). The 23 years (1983–2005) of mean spatial distribution of precipitation over the ISM derived from GPCP v2 and CGCMs are represented in Fig. 2. The spatial distribution of maximum precipitation over the head Bay of Bengal (BOB) and along the west coast of India is recorded in GPCP v2.

The ensemble mean monsoon rainfall climatology with respect to their bias for the same period for the seven models is presented in Fig. 2b–h. In general, the spatial distributions of mean precipitation patterns appear to be reasonably well simulated and close to the observation results (Fig. 2a). However, there are significant differences between the rainfall simulated by different ensemble members of each model (results not shown here), indicating that monsoon rainfall could be very sensitive to initial conditions. The models behave differently for most part of the country: an underestimation of rainfall by some models is observed for central Indian region (CI), while an overestimation of rainfall by a different model is noticed for the same region particularly over central India. The model-to-model variability in simulating rainfall is also large over the Indian Ocean region. Mostly, the coupled models such as APCC, PNU, and UHT1 have shown an underestimation of rainfall over heavy-rainfall regions such as the west coast of India, northeast India, and the equatorial Indian regions as represented in Fig. 2b–h.

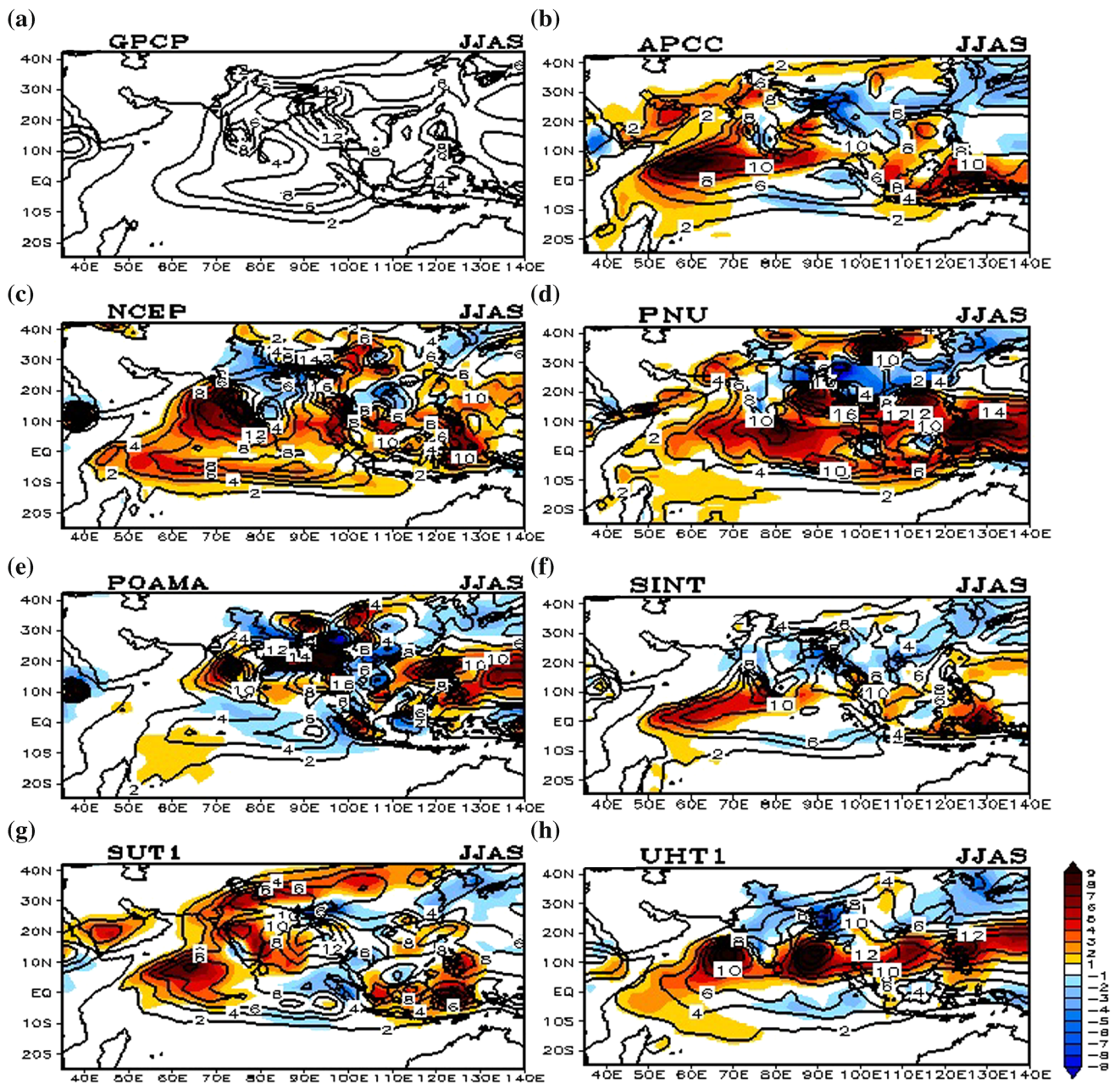


Fig. 2 a–h Spatial distribution of southwest monsoon precipitation (mm d^{-1}) climatology (1983–2005) derived from observation (a) GPCP v2; b–h ensemble mean climatology (counter) and their bias (shaded) of seven CGCMs (APCC, NCEP, PNU, POAMA, SINT, SUT1, and UHT1)

3.2 Interannual variability

Figure 3 shows the percentage departure of monsoonal mean rainfall (mm/season) over land grid points is obtained from two different types of observations viz. IITM rain gauge stations (Parthasarathy et al. 1991) and GPCP v2 compared with CGCMs during the hindcast period to investigate the interannual variability. It has been recognized that the model quality could be evaluated through the retrospective predictions of AISMR to quantify all models and to determine significant fluctuations from the

observation and diverse nature of these models and also to evaluate the dependency with the initial conditions. Although AISMR simulated by these models varies significantly, the predictions with NCEP, POAMA, SINT and SUT1 are relatively more accurate than those with APCC, PNU and UHT1 models.

To quantify the models' fidelity in reproducing the spatial pattern of rainfall climatology, pattern correlation coefficient (PCC) between the rainfall simulated by the models and GPCP v2 is computed. The PCC in terms of interannual variability of precipitation over two different

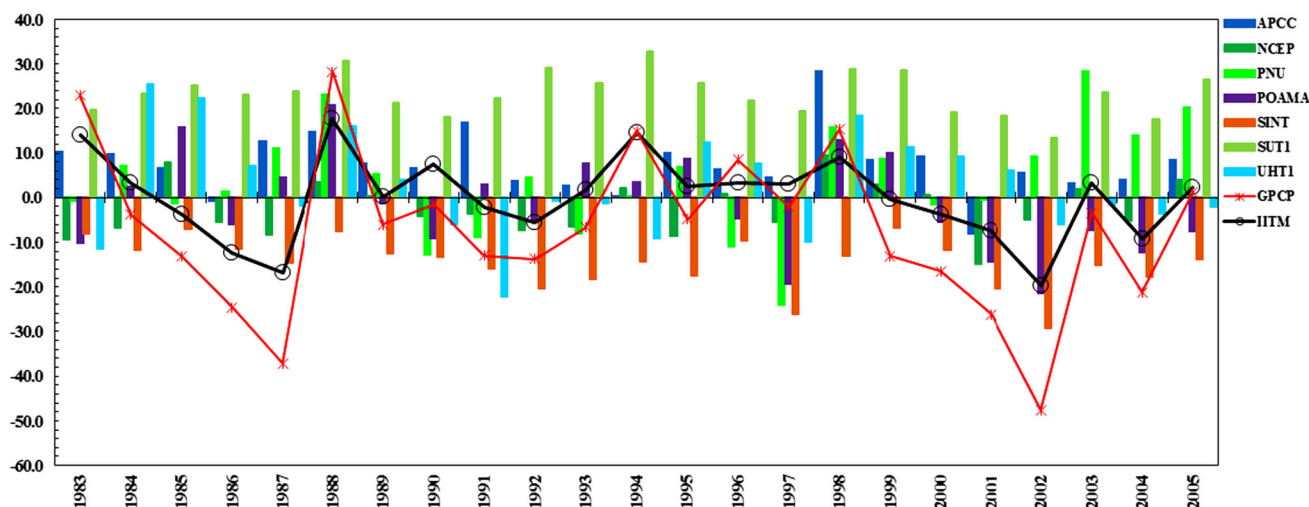


Fig. 3 Comparison of monsoonal rainfall percent departure over Indian land grid point region derived from IITM as well GPCP v2 observations and seven CGCM (APCC, NCEP, PNU, POAMA, SINT, SUT1, and UHT1 mean ensembles)

domains, over the Indian summer monsoon region (ISMR: 20°S–40°N; 40°E–140°E) which includes both land and oceanic grid points and other over an area bounded by (AISMR: 8°–35°N; 68°–98°E) only land grids, is calculated and shown in Table 3. The CGCMs show the highest skill in predicting the spatial pattern of JJAS precipitation over the ISMR, and the mean PCC of these models varies from 0.68 to 0.84 and exhibit uniform characteristics, which is very difficult to quantify the uncertainty for the individual models. To know the prediction skills of AISMR, the mean PCC is calculated for AISMR domain, which varies in the range of 0.06–0.64, indicates a large variation in the model fidelity for the AISMR. Similar types of results for DEMETER-coupled models and CFS were discussed in detail in the previous studies (Preethi et al. 2010; Gadgil and Srinivasan 2011; Acharya et al. 2011a, b). Interestingly, the AISMR has shown larger variability in terms of seasonal to intra-annual time scale (Parthasarathy et al. 1994; Kumar et al. 1995). The year-to-year model fidelity in terms of PCC, as presented in Table 3, shows that models APCC, SINT, SUT1, POAMA and NCEP, have particularly better PCC than PNU and UHT1 models. However, the PCC reproduction is consistently better in neutral and La Niña years than in the El Niño years. In this study, the predictability of the coupled GCMs on the basis of ocean–atmosphere interaction over the Pacific Ocean was evaluated during the El Niño years only, but not during La Niña years. The source of the deficient rainfall during JJAS period over the Indian region arises due to the warming phase of the SST anomaly over the equatorial tropical Pacific region, which has an adverse effect on the agriculture (Gadgil et al. 2005). Therefore, the El Niño teleconnection with AISMR has been explored in detail.

3.3 Anomalous features of El Niño composites and its influence on Indian summer monsoon

(a) SST and Precipitation

For the hindcast period of 1983–2005, six El Niño events occurred during Indian summer monsoon (JJAS) season and these events are characterized by warm SSTA over Niño 3.4 region ≥ 0.45 °C its standard deviation followed by Trenberth (1997). The composites of SST (°C) and precipitation (mm/day) anomaly are analyzed through observation as well with CGCMs and are presented in Figs. 4 and 5. Importantly, the seasonal anomaly was calculated on the basis of the 1983–2005 climatology and the El Niño years are identified through Niño 3.4 index (Trenberth 1997). The SSTA obtained from ERSST shown in Fig. 4a, shows warm SSTA more than 1.0 °C in the central tropical Pacific that extended towards eastern equatorial Pacific region. Figure 5a shows maximum surplus precipitation anomaly also noticed over the equatorial central Pacific region and in the region extending from west to northwest of the equatorial Pacific region. However, positive precipitation anomalies are also seen over the Myanmar, Thailand, Laos, Vietnam, South China Sea (SCS) and adjoining region, which coincides with the warm SSTA. Significantly, warming over Niño 3.4 region closely aligned with the monsoonal precipitation over the tropical region, particularly between 10.0°N–10.0°S and 160.0°E–180.0°E. Simultaneously, strong negative precipitation anomaly is noticed over the Indonesian region. However, moderate to deficient precipitation is observed over Indian peninsula through the Bay of Bengal (BOB) and the adjoining Indian seas. The aforementioned precipitation and SSTA simulated by all models shows that the

Table 3 The root mean square error (RMSE) and spatial correlation coefficients of JJAS precipitation climatology between GPCP v2 and CGCMs ensembles mean over the ISRM and AISMR grid points

MODEL Region	RMSE between GPCP v2 and individual CGCMs		Pattern correction coefficients (PCC) between GPCP v2 and individual CGCM	
	ISMR (20°S–40°N; 40°–140°E)	AISMR (8°–35°N; 68°–98°E)	ISMR (20°S–40°N; 40°–140°E)	AISMR (8°–35°N; 68°–98°E)
APCC	2.24	2.80	0.7	0.37
NCEP	2.71	3.37	0.81	0.43
PNU	3.39	3.84	0.68	0.15
POAMA	3.1	3.61	0.75	0.48
SINT	1.8	1.98	0.84	0.64
SUT1	2.8	3.04	0.78	0.49
UHT1	3.69	3.77	0.73	0.06

model variability over the Pacific is less than Indian Ocean. The surplus negative precipitation anomaly distributions over the maritime continent region particularly Indonesian region are well simulated by NCEP and POAMA as shown in Fig. 5c, e and this agrees well with the GPCPv2. However, moderate to poor prediction is obtained from other five models SINT, SUT1, PNU, APCC, and UHT1. The warm phase of ENSO is associated with the weakening of the Indian monsoon, i.e., on overall reduction in precipitation, which is well represented by the four models PNU, POAMA, SINT, and UHT1, whereas APCC and NCEP models are unable to reproduce the adverse influence of El Niño on AISMR, but the anomaly features are shifted to the west coast of India, particularly over the Arabian Sea in the NCEP model.

(b) Winds at 850 hPa

Composite winds at 850 hPa level during the JJAS season of the El Niño's are depicted from observation and CGCMs to evaluate the dynamical linkage of cyclonic and anticyclonic features significantly associated with North West Pacific (NWP) convection, which is due to the warming over the east to central part of the equatorial Pacific region. Previous studies by Hoskins and Karoly (1981) and Nitta (1987) have shown that interactions between the tropical convection and the wind anomalies can generate and maintain large-scale anomaly patterns of alternating highs and lows that extend meridionally from the equatorial region into the subtropics and mid-latitudes through wave dispersion (Mujumdar et al. 2007). Furthermore, the meridional dispersion of Rossby waves is well known to be strongly enhanced in a belt of westerlies located over the region of anomalous convection (Hoskins and Karoly 1981; Lau and Lim 1984; Chang and Webster 1990); therefore, we examined the wind composites of six El Niño events at 850 hPa derived from NCEP/DOE-II reanalysis (Kanamitsu et al. 2002a, b). In the observation (Fig. 6a) shown that a low-level strong southwesterly wind

anomalies originate from the Maritime continent region between 120°E and 150°W, in addition to its anticyclonic circulation is also observed along the Japan coast, which reduces the convection over that region (Fig. 5a). However, an elongated structure of cyclonic circulation tilted towards the northeast direction and its vicinity persists at 35.0°N–170°E, which could be attributed to suppressed convection over the East–west Pacific rim (illustrated in Fig. 6a). Note that the meridional circulation pattern is characterized by an intensified cyclonic anomaly over the Northwest Pacific region. In fact, coupled GCM prediction provides support indicating that the enrichment of low-level westerlies and easterlies over the Indo-Pacific rim favored enhanced convection in the region, which agrees with the observations. However, among these CGCMs, NCEP, POAMA, SINT, SUT1, and APCC exhibit the best capability in the terms of anomalous features such as cyclonic and anticyclonic patterns attributed with warming through SSTA (shown in Fig. 4b–h), but the position of the cyclonic and anticyclonic features is not identified similar to the observation. Thus, the enhanced precipitation over the Northwest Pacific was sustained due to cyclonic activity (Pradhan et al. 2011; Kim et al. 2011; Kumar and Krishnan 2005) and due to significantly decreased and increased cyclonic activity over the region. In turn, these strong ascending motions over the Northwest Pacific force subsidence and rainfall reduction over the Indian subcontinent through anomalous east–west circulation in between 10°N and 20°N (Fig. 5a). Thus, the convection variability over the Northwest Pacific can be serving as an important component, which determines the ENSO–monsoon teleconnection dynamics (Mujumdar et al. 2007; Ashok et al. 2012). This mechanism is also noted to be operating on intraseasonal timescale for initiating extended monsoon breaks over Central India and eventually creating droughts (Prasanna and Annamalai 2012). In addition, the maximum strength of the monsoon flow pattern over the Arabian Sea is located near 10°–15°N and along 55°–65°E in NCEP,

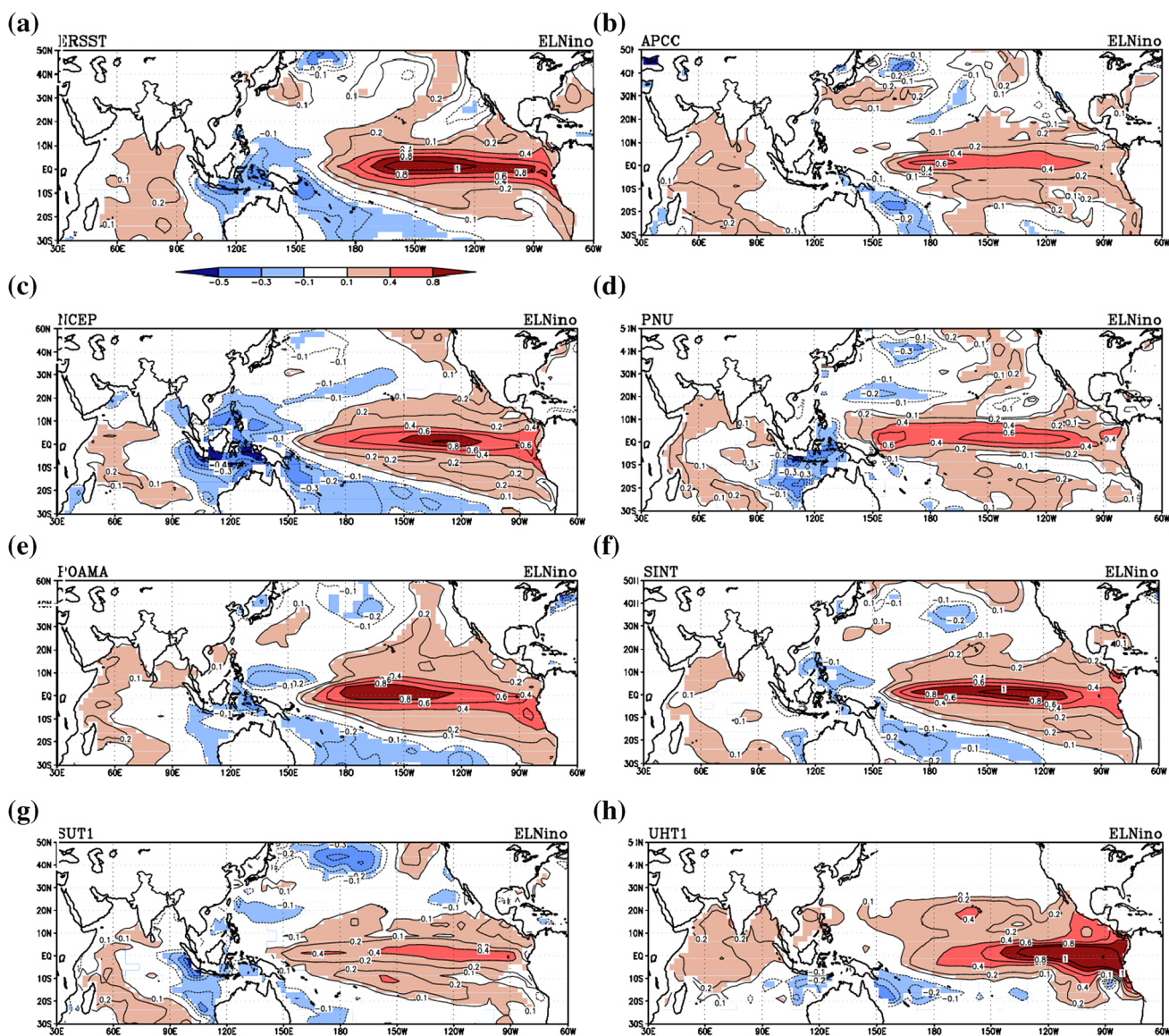


Fig. 4 a NOAA SSTA composites of JJAS ($^{\circ}\text{C}$) for El Niño years (1987, 1991, 1994, 1997, 2002, and 2004); and figures **b–h** same as **a** but, derived from seven CGCMs (APCC, NCEP, PNU, POAMA,

SINT, SUT1, and UHT1). Significant values at 70, 80, and 90 % confidence level are shown by the *different shadings*

POAMA, SINT, and SUT1, which is also close to the observations Fig. 6a.

(c) Evolution of SST and precipitation over the Indo-Pacific rim during El Niño events

Prior to evaluating the monsoon–ENSO relationship, we attempted to evaluate the monthly amplitude of ENSO characteristics with CGCMs, in particular SST and associated precipitation anomalies along the equatorial Pacific region, and thus, circulation anomalies are linked with tropical Pacific up to the Indian monsoon domain. The spatial evolution of tropical Pacific SST and precipitation anomalies are crucial factors for determining the fidelity of

a model (Annamalai et al. 2007). Figure 7 presents a comparison between the observed composite evolutions of Niño-3.4 SST anomalies on a monthly scale starting from June to September, for El Niño events and the similar composites are obtained from the seven CGCMs mean ensembles. It is clearly seen that in observation, maximum warming was found in the year of 1987 and 1997 rather than other El Niño years as simulated by most of the models, but APCC and SUT1 could not predict the same as in Fig. 7a. The eastward movements of the warmest SSTA accompanied by an eastward migration of convection into the central Pacific and cooling SSTA were associated with the suppression of convection over the Maritime Continent

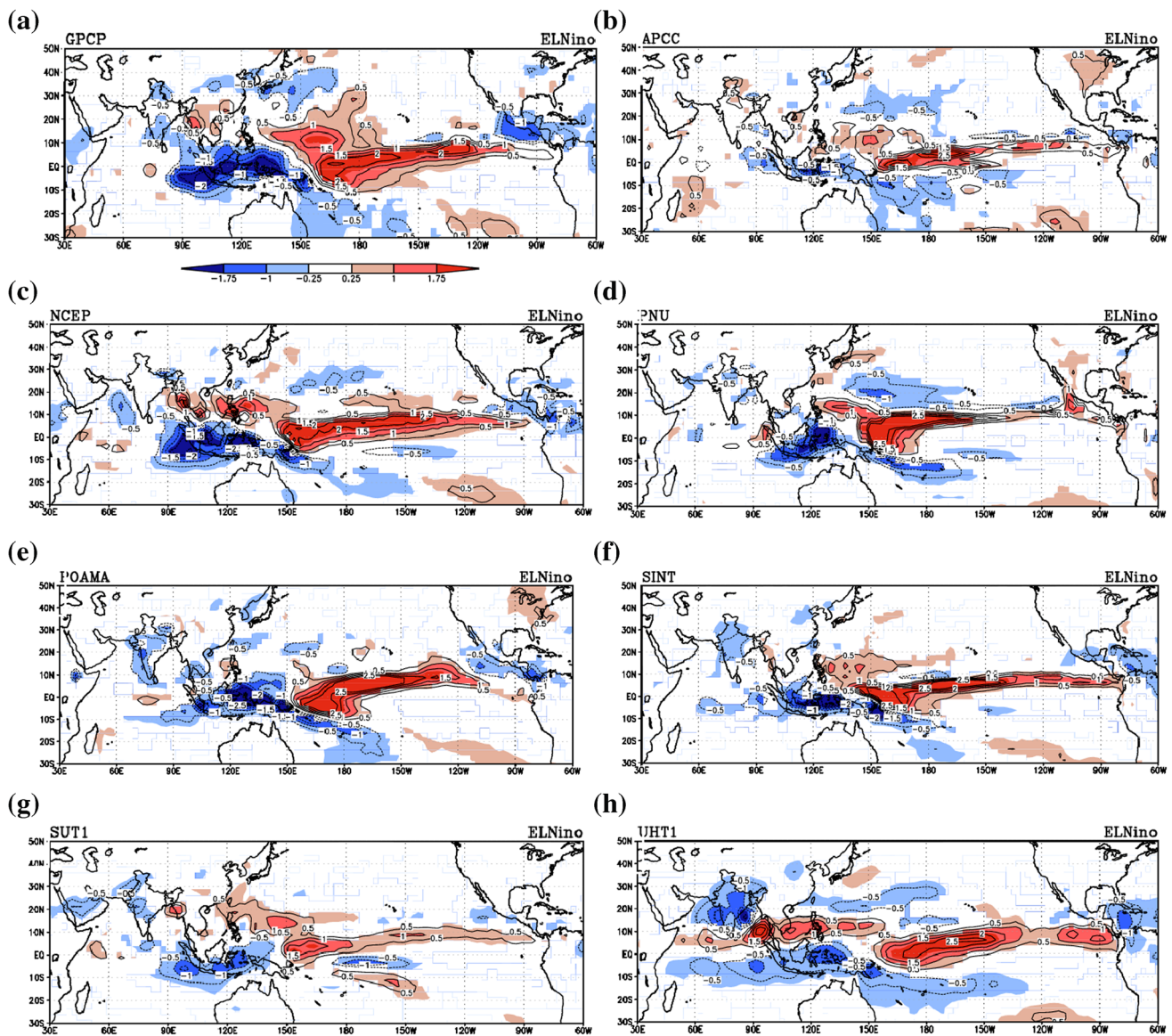


Fig. 5 a–h Same as Fig. 4 except for JJAS precipitation (mm d^{-1}). Significant values at 70, 80, and 90 % confidence level are shown in *shadings*

during the El Niño years, as noticed in the observation (Fig. 8a). This is one of the important features of El Niño events, which is not clearly identified through the CGCMs. The warm SSTa over the equatorial Pacific region, around 160°W – 90°W is clearly represented in NCEP, SINT, POAMA, and SUT1. However, the location of cooling over the Indian Oceanic region, identified by the models did not agree with the observation during JJAS of 1987, 1994 and 1997; this may be the cause why all models fail to predict the AISMR in the years 1994 and 1997. The comparison of observed precipitation anomaly and the precipitation anomaly from all models during the El Niño events shows that NCEP and POAMA models are better performing than other models which is also evident with SST anomaly patterns (Fig. 6a).

4 Hindcast skills for evaluating ENSO and AISMR teleconnection

The spatial patterns of temporal correlation coefficient (TCC) between observed Niño 3.4 indexes obtained from NOAA SST with GPCP v2 precipitation for JJAS period during 1983–2005 are illustrated in Fig. 9a. The TCC from observation shows the strongest to moderate negative scores over the Maritime Continents and Indian region; however, positive TCC is noticed around Myanmar, Thailand, Cambodia and adjoining southern parts of China. In addition, the strong positive TCC scores are seen over the equatorial Pacific region maximum at 2.5°N – 180°E in the observations. The representation of simultaneous impact of SSTA over the Niño 3.4 region of the tropical Pacific region and

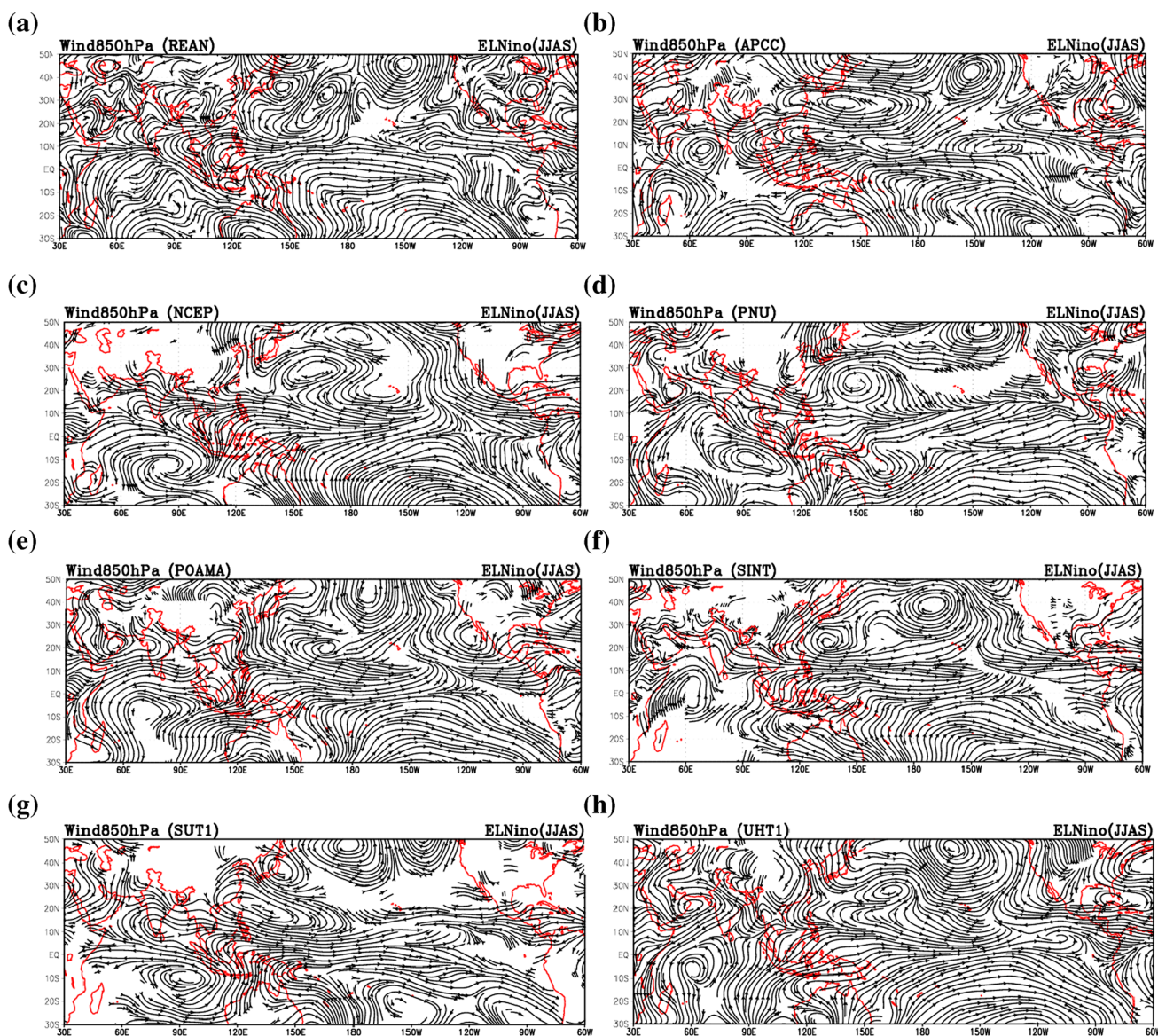


Fig. 6 a NCEP-Reanalysis-II composites of JJAS wind at 850 hPa (ms^{-1}) anomaly for El Niño years (1987, 1991, 1994, 1997, 2002, and 2004); figures b–h same as a but, from seven CGCMs (APCC, NCEP, PNU, POAMA, SINT, SUT1 and UHT1)

their influence on precipitation indicates the adverse influence for AISMR. This is one of the important characteristics of El Niño that shows the natural sensitivity to the India's monsoon epochs during JJAS period (Kumar et al. 2011).

The teleconnection characteristics between ENSO and Indian summer monsoon rainfall have been well known (Goswami and Xavier 2005; Krishnamurthy and Goswami 2000; Kumar et al. 1999, 2006), and studies through CGCMs have been conducted by several researchers (Webster et al. 1991, 1992; Achuta Rao and Sperber 2002; Annamalai et al. 2007; Preethi et al. 2010; Rajeevan et al. 2012; Chaudhari et al. 2012; Joseph et al. 2012). To evaluate the prediction skill of the CGCMs, it is necessary to quantify the SSTA over the Niño 3.4 region in the

Pacific Ocean. Thus, to have a quantitative measurement of the forecast skill, the temporal correlation coefficient (TCC) calculated at each grid point has been considered here (Table 4). The spatial patterns of TCC between observed Niño 3.4 obtained from ERSST with GPCP v2 precipitation during 1983–2005 are shown in Fig. 9a. Similarly, the TCC score of simulated Niño 3.4 index and the global precipitation from seven CGCMs is also presented in the Fig. 9b–h for a comparison with the observation. The TCC from the observation shows the strong and moderate negative scores over the Maritime Continents and Indian region, but positive TCC occurs in and around Myanmar, Thailand, Cambodia, and adjoining southern parts of China. In addition to it, strong positive TCC scores

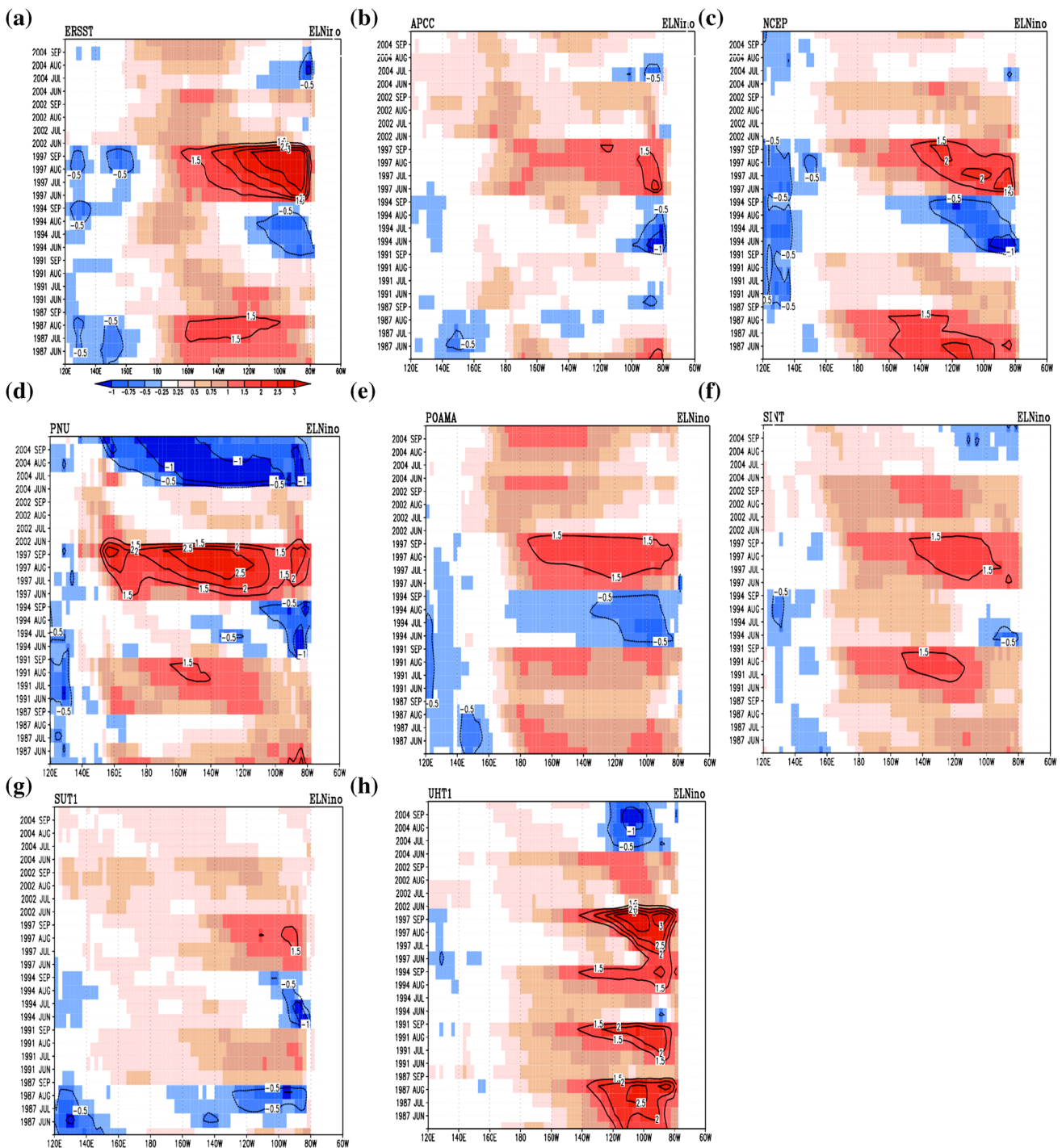


Fig. 7 Evolution of SST anomaly ($^{\circ}\text{C}$) through June to September over the Indo-Pacific region [area average of (5°S – 5°N)] during six El Niño events (1987, 1991, 1994, 1997, 2002, and 2004)

(a) observation; (b–h) from coupled GCMs (APCC, NCEP, PNU, POAMA, SINT, SUT1, and UHT1)

occur over the equatorial Pacific region, maximum at 2.5°N – 180°E , in the observations. This representation of SSTa over the Niño 3.4 tropical Pacific region and precipitation anomalies indicates the inverse relationship for ISMR and thus causes weakening of AISMR. Figure 9b–h also indicates TCC score from the CGCMs and most of the

CGCMs show the negative TCC scores over the maritime continent, particularly over the Philippines Sea and the adjoining region, which is in agreement with the observational result. The skills over the Philippines Sea as simulated using CGCMs, particularly NCEP, POAMA, SINT, and UHT1 agree well with the observation, whereas the

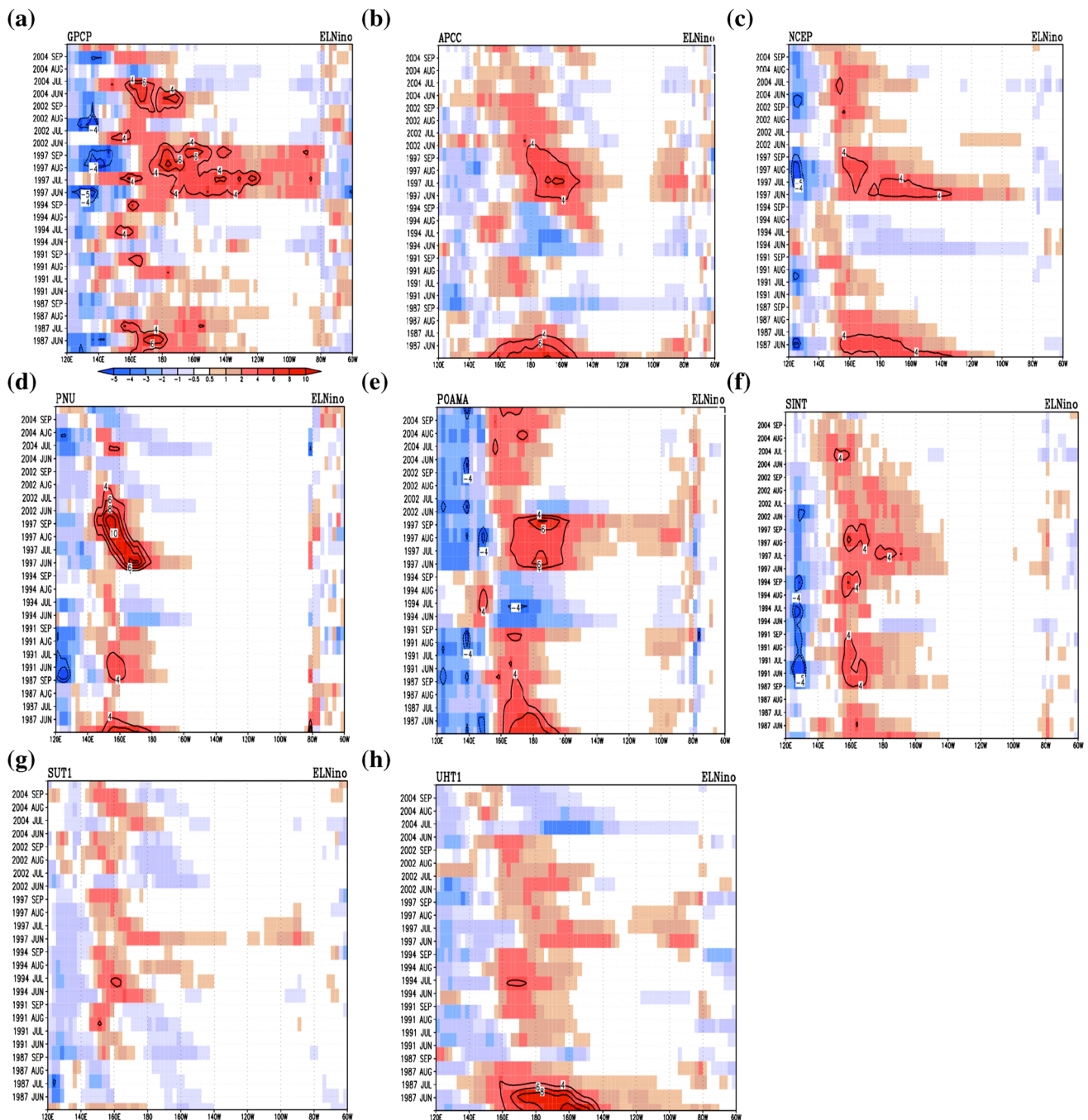


Fig. 8 Evolution of precipitation anomaly (mm/day) for JJAS period over the Indo-Pacific region [area average of (5°S – 5°N)] during six El Niño events (1987, 1991, 1994, 1997, 2002 and 2004) (a) observation;

(b–h) from coupled GCMs (APCC, NCEP, PNU, POAMA, SINT, SUT1, and UHT1)

agreement is poor in the case of APCC, PNU and SUT1. The main significant features of the negative and positive TCC over the East and West Indian Ocean are identified by observations and are clearly reflected in NCEP as well as POAMA. However, there is no similar TCC signal captured by NCEP over peninsular India (Karnataka) region, whereas POAMA overestimates in the northwest (Gujarat) and northeast (Assam) parts of India.

5 Proposal of MME for AISMR prediction

As discussed in the previous sections, the individual CGCMs performance is evaluated in terms of climatology and their biases. Composite analysis and monthly evolution of the anomalous SST and precipitation over the equatorial Indo-Pacific rim are used to conclude that the models APCC, NCEP, POAMA, SINT and SUT1 show better

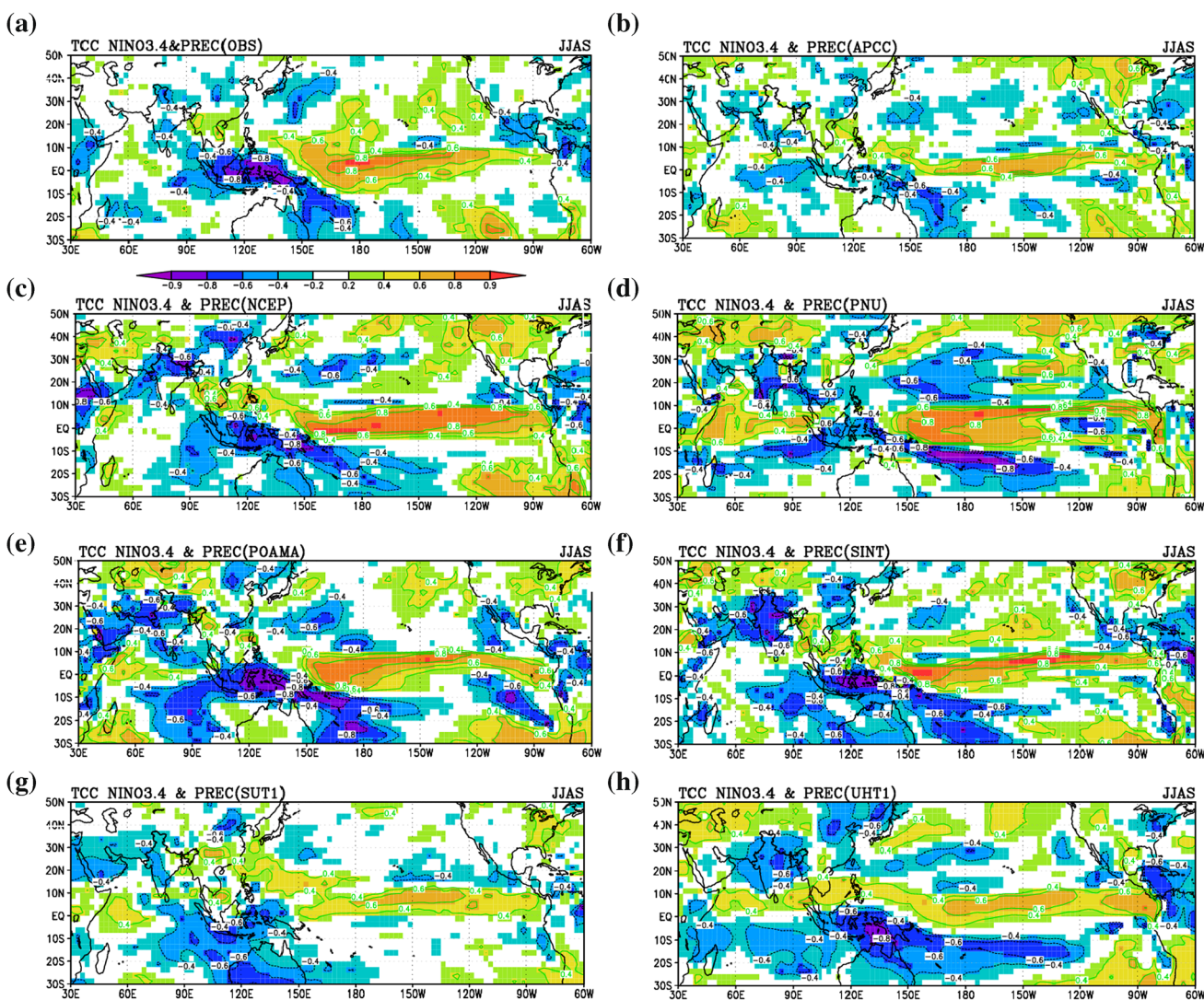


Fig. 9 Temporal correlation coefficients (TCC) between Niño 3.4 index and global precipitation anomaly during JJAS period derived from observation and seven CGCMs (APCC, NCEP, PNU, POAMA, SINT, SUT1, and UHT1)

Table 4 Same as Table 1 but values are obtained from individual CGCMs

Models	1-month lead forecast of ENSO and AISMR relationships
APCC	-0.24
NCEP	-0.60
PNU	-0.57
POAMA	-0.66
SINT	-0.64
SUT1	-0.60
UHT1	-0.78
MME1	-0.76
MME2	-0.62

skills. Keeping this in mind, we propose two kinds of MME of these CGCMs based on simple composite method (SCM) followed by Min et al. (2014). The detailed methodology of constructing composites using SCM is dealt in Min et al. (2014).

First, we consider seven CGCMs (APCC, NCEP, PNU, POAMA, SINT, SUT1, and UHT1) to construct a MME referred to as MME1; similarly, MME2 is constructed using five CGCMs APCC, NCEP, POAMA, SINT, and SUT1, respectively. Then, their performance in predicting the remote climate influence such as ENSO and ISMR is evaluated. The analysis performed using the MME1 and MME2 shows better TCC scores of Niño 3.4 index with precipitation and subsequently AISMR with global SST

appears to be close to the observation. Significant improvements in TCC skills are shown in MME1 and MME2 as compared to the individual CGCMs. The positive (negative) scores of TCC over the Northwest Pacific (adjoining Japan) region became weak in MME2 than in MME1, while this asymmetric condition is incorporated with cyclonic and anti-cyclonic features (Figure not shown). In addition, the negative TCC skill over the Indian peninsula reduced by around 15 % through MME2 than MME1 and better skill seems to be over the North East Indian region. However, the TCC score of MME2 is closer to the observation result than those of MME1 as well individual CGCMs.

The standardized anomaly of simulated Niño3.4 SST and AISMR from the seven coupled models for the retrospective 23-year period shows that the major ENSO

conditions like those for 1987/1988, 1997/1998 and 2002/2003 agree well with observation, which indicates that CGCMs have credibility in representing the climate indices over the tropical Pacific region shown in Table 4. The CC of CGCMs with observation is highly statistically significant above 90.0 % level except in the case of PNU model. However, the warm phase of ENSO condition during 1987 and 2002 could not be simulated by UHT1 but similar features are captured by all other CGCMs. The MME1 and MME2 performed better than individual CGCMs, and their spatial CC is relatively higher than the observational result (-0.48); in fact, the ENSO and ISMR teleconnection in MME2 is -0.62 , whereas in MME1 is -0.76 , respectively. Moreover, the hindcast prediction through MME1 and MME2 of AISMR and their comparison with IITM observation shows that the CC of MME2

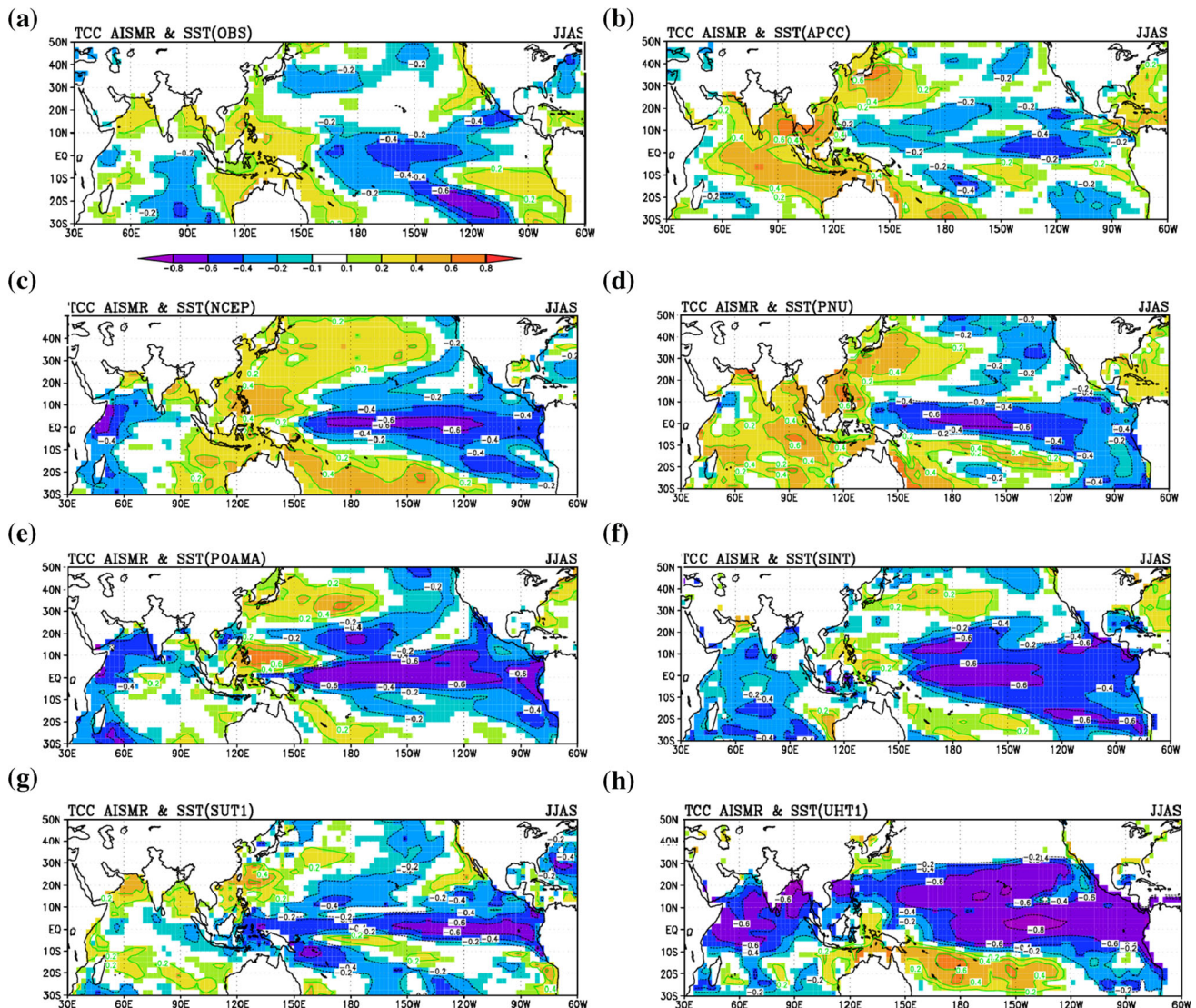


Fig. 10 Temporal correlation coefficients (TCC) between AISMR and global SST anomaly during JJAS period derived from observation and coupled GCMs (APCC, NCEP, PNU, POAMA, SINT, SUT1, and UHT1)

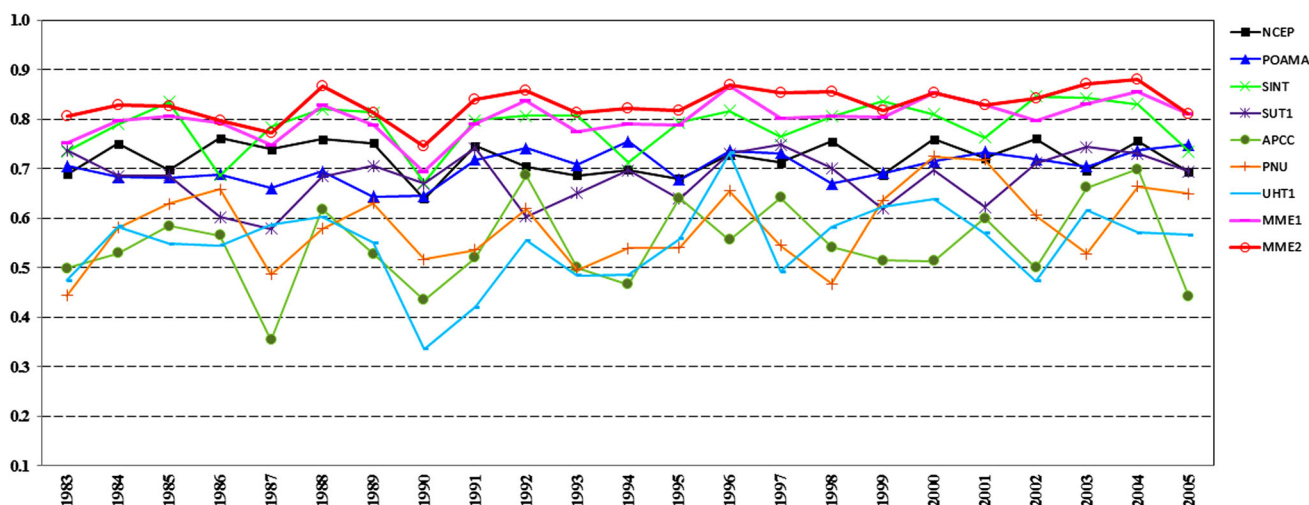


Fig. 11 Anomaly correlation coefficients (ACC) of AISMR between GPCPv2 and seven CGCMs, MME1 and MME2

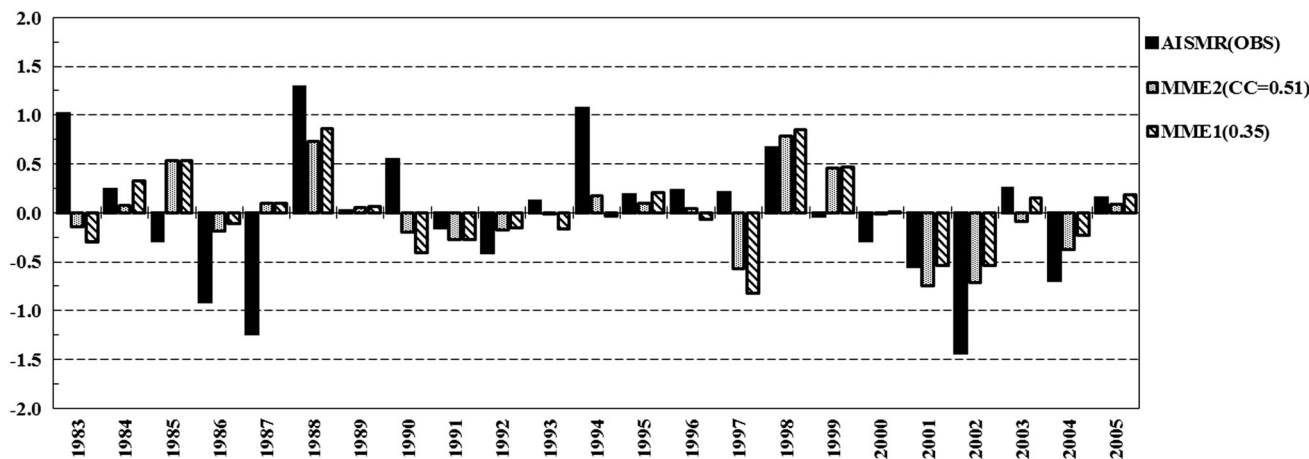


Fig. 12 Time series of normalized AISMR from OBS, MME1 and MME2 during the hindcast period of 1983–2005

(prediction skill) is better than that of MME1; their CC values are around 0.51 and 0.35, respectively (see Fig. 10).

The anomaly correlation coefficients (ACC) between GPCPv2 and seven individual ensemble forecast of AISMR derived from the CGCMs following (Kar et al. 2011) are presented in Fig. 11. Figure 11 shows that four models viz. APCC, NCEP, POAMA, SINT, and SUT1, the ACC varies in the range between 0.35 and 0.88. However, the ACC varies from 0.35 to 0.7 for PNU and UHT1 models. Thus, we notice that the MME prediction of AISMR from all CGCMs and with five best CGCMs differs substantially. The results are encouraging and predictive skills of both MME1 and MME2 are better than the individual CGCMs. Interestingly, 1994 and 1997 were El Niño years, but the AISMR recorded moderate to normal rainfall due to influence of positive IOD, the ACC is better represented in MME2 than in MME1. In addition, Fig. 12 summarizes the skill of seasonal prediction for AISMR of individual models as well as MME1 and MME2.

Precipitation in MME2 shows significantly better skills than MME1 and relatively close to observation. Figure 13 summarizes the pattern correlation coefficient of individual models over ISMR, AISMR and CI. MME2 shows a better pattern correlation coefficient compared to MME1. Among the seven models, SINT has the highest pattern correlation of precipitation over the Indian monsoon region; moreover, the pattern correlation is above 0.5, when we consider a small land region of central India (Rajeevan et al. 2004 CI) (Fig. 13). The central Indian region is the most important region for capturing the summer monsoon dynamics.

6 Conclusions and discussion

The prime objective of this work is to evaluate the skill of seven CGCMs, which are currently semi-operational at APCC since 2009 in predicting ISMR. The strength of ISMR represented by AISMR, and its interannual

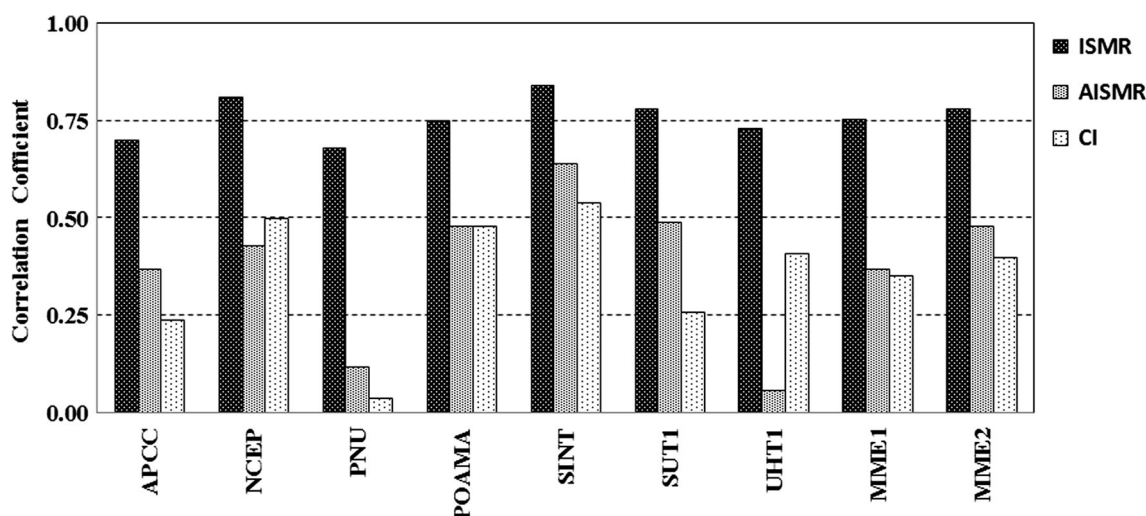


Fig. 13 Pattern correlation coefficient(PCC) of precipitation over ISMR, AISMR and CI region derived from seven coupled GCMs, MME1 and MME2 during hindcast period of 1983–2005

variability is associated with the characteristics of SSTA over the central-eastern Pacific such as the Niño 3.4 region. Therefore, the amplitude of ENSO and the variability of AISMR derived from the observed and retrospective prediction of coupled GCMs such as APCC, NCEP, PNU, POAMA, SINT, SUT1, and UHT1 during JJAS period starting from 1983 to 2005 with May initial condition, in other words 1-month lead prediction, has been documented in this work.

The southwest monsoon precipitation derived from the ensemble mean of the individual CGCMs result shows the systematic biases in the representation of mean monsoon seasonal precipitation over the Indian region. Among the seven models, SINT has the highest pattern correlation of precipitation over the Indian monsoon region. SINT model performs the best over this region compared to other models as it is evident from Figs. 4, 8, 9 and 13. The teleconnection pattern revealed by SINT model is superior to any other individual model.

The prediction of the spatial distribution of precipitation over the northeast and west coast of India through five models (MME2) such as APCC, NCEP, POAMA, SINT, and SUT1 is better with a prediction skill of around 48 %. The biases in most of the individual CGCMs are similar and the correction of the inherent bias in the mean state is critical for improving in one-month lead-time forecast. Interestingly, the remote forcing over the Pacific such as the warm phase of ENSO and its coupling with Indian summer monsoon prediction is robust with CGCMs; however, the SSTA over the tropical Indian Oceanic region (dipole mode) is associated by ENSO (Ashok et al. 2004) and also influences AISMR; thus, their predictions and skills are relatively poor as compared to the ENSO prediction. The ENSO amplitudes analyzed through the Niño

3.4 index and the standardized anomaly correlation coefficient with observation and coupled GCMs particularly APCC and UHT1 showed poorer performance than other CGCM models. The poor performance of individual CGCM also affects the MME technique (DelSole and Shukla 2012). To quantify this issue, we tested two types of MME schemes viz. MME1 and MME2 with and without two underperforming CGCMs. The ACC shows that MME2 is better than MME1. We plan to extend this study for the prediction of IOD events.

Acknowledgments The authors sincerely thank Director of APEC Climate Center (APCC), Busan, Republic of Korea, for providing opportunity and necessary facilities to carry out this study. The authors also would like to acknowledge data centers for providing observation and reanalysis fields to evaluate the coupled Global Climate Models (GPCPv2, NOAA and NCEP/NCAR). We sincerely acknowledge COLA, USA for providing their software GrADs, in which figures are prepared and used in this paper.

References

- Abrol YP, Gadgil S (1999) Rice- in a variable climate. APC Publications Pvt Ltd, New Delhi, p 243
- Acharya N, Kar SC, Mohanty UC, Kulkarni MA, Dash SK (2011a) Performance of GCMs for seasonal prediction over India—a case study for 2009 monsoon. *Theor Appl Climatol* 105(3–4):505–520. doi:10.1007/s00704-010-0396-2
- Acharya N, Kar SC, Kulkarni MA, Mohanty UC (2011b) Multi-model ensemble schemes for predicting northeast monsoon rainfall over peninsular India. *J Earth Syst Sci* 120:795–805
- Achuta Rao K, Sperber KR (2002) Simulation of the El Niño southern oscillation: results from the coupled model intercomparison project. *Clim. Dyn* 19:191–209
- Adler RF, Huffman GJ, Chang A, Ferraro R, Xie P, Janowiak J, Rudolf B, Schneider U, Curtis S, Bolvin D, Gruber A, Susskind J, Arkin P (2003) The version 2 global precipitation climatology project (GPCP) monthly precipitation analysis (1979–present). *J Hydrometeorol* 4:1147–1167

- Ailikun B, Yasunari T (2001) ENSO and Asian summer monsoon: persistence and transitivity in the seasonal march. *J Meteorol Soc Jpn* 79:145–159
- Annamalai H, Slingo JM, Sperber KR, Hodges K (1999) The mean evolution and variability of the Asian summer monsoon: comparison of ECMWF and NCEP–NCAR reanalysis. *Mon Weather Rev* 127:1157–1186
- Annamalai H, Hamilton K, Sperber KR (2007) The south Asian summer monsoon and its relationship with ENSO in the IPCC AR4 simulations. *J Clim* 20:1071–1092
- Ashok K, Guan Z, Yamagata T (2001) Impact of the Indian Ocean dipole on the relationship between the Indian monsoon rainfall and ENSO. *Geophys Res Lett* 26:4499–4502
- Ashok K, Chan W-L, Motoi T, Yamagata T (2004) Decadal variability of the Indian Ocean dipole. *Geophys Res Lett* 31:L24207
- Ashok K, Sabin TP, Swapna P, Murtugudde RG (2012) Is a global warming signature emerging in the tropical Pacific. *Geophys Res Lett* 39:L02701
- Barnett TP (1984) Prediction of the El-Niño of 1982–83. *Mon Wea Rev* 112:1403–1407
- Barnston AG, Michael KT, Michelle LL'H, Shuhua Li, David GD (2012) Skill of real-time seasonal ENSO model predictions during 2002–11: is our capability Increasing? *Bull Amer Meteor Soc* 93:631–651
- Behera SK, Krishnan R, Yamagata T (1999) Unusual ocean-atmospheric conditions in the tropical Indian Ocean during 1994. *Geophys Res Lett* 26:3001–3004
- Branković Č, Palmer TN, Molteni F, Tibaldi S, Cubasch U (1990) Extended-range predictions with ECMWF models: time-lagged ensemble forecasting. *Q.J.R Meteorol Soc* 116:867–912. doi:10.1002/qj.49711649405
- Brankovic C, Palmer TN (2000) Seasonal skill and predictability of ECMWF PROVOST ensembles. *Q J R Meteorol Soc* 126:2035–2067
- Boschat G, Terray P, Masson S (2012) Robustness of SST teleconnections and precursory patterns associated with the Indian summer monsoon rainfall. *Clim Dyn* 38(11–12):2143–2165
- Chakraborty A, Krishnamurti TN (2006) Improved seasonal climate forecasts of the south Asian summer monsoon using a suite of 13 coupled ocean-atmosphere models. *Mon Wea Rev* 134:1697–1721
- Chang H-R, Webster PJ (1990) Energy accumulation and emanation at low latitudes. Part II: Nonlinear response to strong episodic forcing. *J Atmos Sci* 47:2624–2644
- Charney JG, Shukla J (1981) Predictability of monsoons. In: Lighthill J, Pearce RP (eds) *Monsoon dynamics*. Cambridge University Press, Cambridge, pp 99–108
- Chaudhari HS, Pokhrel S, Saha SK, Dhakate A, Yadav RK, Salunke K, Mahapatra S, Sabeerali CT, Rao SA (2012) Model biases in long coupled runs of NCEP CFS in the context of Indian summer monsoon. *Int J Clim* 33(5):1057–1069
- DelSole T, Shukla J (2012) Climate models produce skillful predictions of Indian summer monsoon rainfall. *Geophys Res Lett* 39:L09703. doi:10.1029/2012GL051279
- Fu X, Wang B (2004) Differences of boreal summer intraseasonal oscillations simulated in an atmosphere–ocean coupled model and an atmosphere-only model. *J Clim* 17:1263–1271
- Gadgil S (1995) Climate change and agriculture—an Indian perspective. *Curr Sci* 69:649–659
- Gadgil S, Sajani S (1998) Monsoon precipitation in the AMIP runs. *Clim Dyn* 14:659–689
- Gadgil S, Vinayachandran PN, Francis PA, Gadgil S (2004) Extremes of the Indian summer monsoon rainfall, ENSO and equatorial Indian Ocean oscillation. *Geophys Res Lett* 31:L12213. doi:10.1029/2004GL019733
- Gadgil S, Rajeevan M, Nanjundiah R (2005) Monsoon prediction: why yet another failure? *Curr Sci* 88:1389–1400
- Gadgil S, Srinivasan J (2011) Seasonal prediction of the Indian monsoon. *Curr Sci* 1003:343–353
- Gershunov Alexander, Schneider Niklas, Barnett Tim (2001) Low-frequency modulation of the ENSO–Indian monsoon rainfall relationship: signal or noise? *J. Climate* 14:2486–2492
- Goswami BN, Jayavelu V (2001) On possible impact of the Indian summer monsoon on the ENSO. *Geophys Res Letts* 28(4):571–574
- Goswami BN, Xavier PK (2005) ENSO control on the south Asian monsoon through the length of the rainy season. *Geophys Res Lett* 32:L18717. doi:10.1029/2005GL023216
- Ham Y-G, Kang I-S (2011) Improvement of seasonal forecasts with inclusion of tropical instability waves on initial conditions. *Clim Dyn* 36(7–8):1277–1290
- Hoskins BJ, Karoly DJ (1981) The steady linear response of a spherical atmosphere to thermal and orographic forcing. *J Atmos Sci* 38:1179–1196
- Janakiraman S, Ved M, Laveti RN, Yadav P, Gadgil S (2011) Prediction of the Indian summer monsoon rainfall using a state-of-the-art coupled ocean-atmosphere model. *Curr Sci* 100(3):354–362
- Jeong HI, Ashok K, Song BG, Min Y-M (2008) Experimental 6-month hindcast and forecast simulations using CCSM3, APCC 2008 Technical Report, APEC Climate Center
- Jeong HI, Doo YL, Ashok K, Joong-Bae A, June-Yi L, Jing-Jia L, Jae-Kyung ES, Harry HH, Karl B, Yoo-Geun H (2012) Assessment of the APCC coupled MME suite in predicting the distinctive climate impacts of two flavors of ENSO during boreal winter. *Clim Dyn* 39:475–493. doi:10.1007/s00382-012-1359-3
- Joseph S, Sahai AK, Goswami BN, Terray P, Masson S, Luo J-J (2012) Possible role of warm SST bias in the simulation of boreal summer monsoon in SINTEX-F2 coupled model. *Clim Dyn* 34:1561–1576. doi:10.1007/s00382-011-1264-1
- Kanamitsu M, Ebisuzaki W, Woollen J, Yang S-K, Hnilo JJ, Fiorino M, Potter GL (2002a) NCEP–DOE AMIP-II reanalysis (R-2). *Bull Am Meteorol Soc* 83:1631–1643
- Kanamitsu M, Kumar A, Juang HMH, Wang W, Yang F, Schemm J, Hong SY, Peng P, Chen W, Ji M (2002b) NCEP dynamical seasonal forecast system. *Bull Am Meteorol Soc* 83:1019–1037
- Kang IS, Jin K, Wang B, Lau KM, Shukla J, Krishnamurthy V, Schubert SD, Waliser DE, Stern WF (2002) Intercomparison of the climatological variations of Asian summer monsoon precipitation simulated by 10 GCMs. *Clim Dyn* 19:383–395
- Kar SC, Acharya N, Mohanty UC, Kulkarni MA (2011) Skill of mean of distribution of monthly rainfall over India during July using multi-model ensemble schemes. *Int J Climatol*. doi:10.1002/joc.2334
- Kim HM, Webster PJ, Curry JA (2011) Modulation of north Pacific tropical cyclone activity by the three phases of ENSO. *J Clim* 24:1839–1849
- Kinter JL, Miyakoda K, Yang S (2002) Recent changes in the connection from the Asian monsoon to ENSO. *J Clim* 15:1203–1214
- Kirtman BP, Shukla J (2000) Influence of the Indian summer monsoon on ENSO. *Q J R Meteorol Soc* 126:1623–1646
- Kripalani RH, Kulkarni A (1999) Climatology and variability of historical soviet snow depth data: some new perspectives in Snow-Indian monsoon teleconnections. *Clim Dyn* 15:475–489
- Krishnan R, Zhang C, Sugi M (2000) Dynamics of breaks in the Indian summer monsoon. *J Atmos Sci* 57:1354–1372
- Krishnamurthy V, Goswami BN (2000) Indian monsoon-ENSO relationship on inter decadal time scales. *J Clim* 13:579–595
- Krishnamurti TN, Kishtawal CM, LaRow TE, Bachiochi DR, Zhang Z, Williford CE, Gadgil S, Surendran S (1999) Improved

- weather and seasonal climate forecasts from multi-model superensemble. *Science* 285:1548–1550
- Kucharski F, Bracco A, Yoo JH, Molteni F (2007) Low-frequency variability of the Indian monsoon–ENSO relationship and the tropical Atlantic: the ‘weakening’ of the 1980s and 1990s. *J Clim* 20:4255–4266
- Kucharski F, Bracco A, Yoo JH, Molteni F (2008) Atlantic forced component of the Indian monsoon interannual variability. *Geophys Res Lett* 35:L04706. doi:10.1029/2007GL033037
- Kumar KK, Soman MK, Kumar KR (1995) Seasonal forecasting of Indian summer monsoon rainfall: a review. *Weather* 50:449–467
- Kumar KK, Rajagopalan B, Cane MA (1999) On the weakening relationship between the Indian monsoon and ENSO. *Science* 284(5423):2156–2159
- Kumar V, Krishnan R (2005) On the association between the Indian summer monsoon and the cyclone activity over Northwest Pacific. *Curr Sci* 88(4):602–612
- Kumar KK, Rajagopalan B, Hoerling M, Bates G, Cane M (2006) Unraveling the mystery of Indian monsoon failure during El Niño. *Science* 314(5796):115–119
- Kumar KK, Kamala K, Rajagopalan B, Hoerling MP, Eischeid JK, Patwardhan SK, Srinivasan G, Goswami BN, Nemanai R (2011) The once and future pulse of Indian monsoonal climate. *Clim Dyn* 36:2159–2170. doi:10.1007/s00382-010-0974-0
- Latif M, Anderson D, Barnett T, Cane M, Kleeman R, Leetmaa A, O’Brien J, Rosati A, Schneider E (1998) A review of the predictability and prediction of ENSO. *J Geophys Res* 103(C7):14375–14393. doi:10.1029/97JC03413
- Lau K-M, Lim H (1984) On the dynamics of equatorial forcing of climate teleconnections. *J Atmos Sci* 41(2):161–176
- Lee J-Yi, Wang B, Kang I-S, Shukla J (2010) How are seasonal prediction skills related to models’ performance on mean state and annual cycle. *Clim Dyn* 35:267–283
- Lorenz EN (1969) The predictability of a flow which possesses many scales of motion. *Tellus* 21:289–307. doi:10.1111/j.2153-3490.1969.tb00444.x
- Luo JJ, Masson S, Behera S, Shingu S, Yamagata T (2005) Seasonal climate predictability in a coupled OAGCM using a different approach for ensemble forecasts. *J Clim* 18:4474–4497
- Min Y-M, Kryjov VN, Oh SM (2014) Assessment of APCC multimodel ensemble prediction in seasonal climate forecasting: retrospective (1983–2003) and real-time forecasts (2008–2013). *J Geophys Res* 119:12132–12150. doi:10.1002/2014JD022230
- Mooley DA, Parthasarathy B (1984a) Fluctuation in all-India summer monsoon rainfall during 1871–1985. *Clim Change* 6:287–301
- Mooley DA, Parthasarathy B (1984b) Indian summer monsoon and El Niño. *Pure Appl Geophys* 121:339–352
- Mujumdar M, Kumar V, Krishnan R (2007) Indian summer monsoon drought of 2002 and its linkage with tropical convective activity over northwest Pacific. *Clim Dyn* 28:743–758. doi:10.1007/s00382-006-0208-7
- Nitta T (1987) Convective activities in the tropical western Pacific and their impact on the northern hemisphere summer circulation. *J Meteorol Soc Jpn* 41:373–390
- Parthasarathy B, Kumar KR, Munot AA (1991) Evidence of secular variations in Indian monsoon rainfall—circulation relationships. *J Clim* 4:927–938
- Parthasarathy B, Munot AA, Kothawale DR (1994) All-India monthly and seasonal rainfall series: 1871–1993. *Theor Appl Climatol* 49:217–224
- Pradhan PK, Ashok K, Preethi B, Krishnan R, Sahai AK (2011) Modoki, IOD and Western North Pacific typhoons: possible implications for extreme events. *J Geophys Res* 116:D18108
- Prasanna V, Annamalai H (2012) Moist dynamics of extended monsoon breaks over south Asia. *J Clim* 25:3810–3831
- Preethi B, Kripalani RH, Krishna Kumar K (2010) Indian summer monsoon rainfall variability in global coupled ocean-atmospheric models. *Clim Dyn* 35:1521–1539
- Rasmusson EM, Carpenter TH (1983) The relationship between eastern equatorial Pacific sea surface temperature and rainfall over India and Sri Lanka. *Mon Weather Rev* 111:517–528
- Rajeevan M, Pai DS, Dikshit SK, Kelkar RR (2004) IMD’s new operational models for long range forecast of southwest monsoon rainfall over India and their verification for 2003. *Curr Sci* 86(3):422–431
- Rajeevan M, Pai DS (2006) On El Niño–Indian monsoon predictive relationships. NCC Research Report 4, Indian Meteorological Department, Pune 411 005
- Rajeevan M, Pai DS, Kumar RA, and Lal B (2007) New statistical models for long-range forecasting of southwest monsoon rainfall over India. *Clim Dyn*. doi:10.1007/s00382-006-019706
- Rajeevan M, Nanjundiah RS (2009) Coupled model simulations of twentieth century climate of the Indian summer monsoon. In: Mukunda N (ed) Current trends in science-platinum jubilee special. Indian Academy of Science, pp 537–567. <http://www.ias.ac.in/academy/pjubilee/book.html>
- Rajeevan M, Unnikrishnan CK, Preethi B (2012) Evaluation of the ENSEMBLES multi-model seasonal forecasts of Indian summer monsoon variability. *Clim Dyn* 38:2257–2274
- Saha S, Nadiga S, Thiaw C, Wang J, Wang W, Zhang Q, Van den Dool HM, Pan HL, Moorthi S, Behringer D, Stokes D, Penã M, Lord S, White G, Ebisuzaki W, Peng P, Xie P (2006) The NCEP climate forecast system. *J Clim* 19:3483–3517
- Saji NH, Goswami BN, Vinayachandran PN, Yamagata T (1999) A dipole mode in the tropical Indian Ocean. *Nature* 401:360–363
- Shukla J, Kirtman BP (1996) Predictability and error growth in a coupled ocean-atmosphere model. *COLA Tech Rep* 24:1–13
- Sikka DR (1980) Some aspects of large-scale fluctuations of summer monsoon rainfall over India in relation to fluctuations in planetary and regional scale circulation parameters. *Proc Ind Acad Sci (Earth & Planetary Sciences)* 89:179–195
- Slingo J (1999) The Indian summer monsoon and its variability. In: Navarra A (ed) Beyond El Niño: decadal and interdecadal climate variability. Springer, Berlin, pp 103–118
- Slingo JM, Annamalai H (2000) 1997: the El Niño of the century and the response of the Indian summer monsoon. *Mon Weather Rev* 128:1778–1797
- Sun J, Ahn J-B (2011) A GCM-based forecasting model for the landfall of tropical cyclones in China. *Adv Atmos Sci* 28:1049–1055. doi:10.1007/s00376-011-0122-8
- Swaminathan MS (1987) Abnormal monsoons and economic consequences: the Indian experiment. In: Fein JS, Stephens PL (eds) Monsoons. Wiley, New York, pp 121–134
- Smith TM, Reynolds RW, Peterson TC, Lawrimore J (2005) Improvements to NOAA’s historical merged land–ocean surface temperature analysis (1880–2006). *J Clim* 21:2283–2296
- Trenberth KE (1997) The definition of El Niño. *Bull Amer Meteorol Soc* 78:2771–2777
- Walker GT (1923) Correlation in seasonal variations of weather. VIII. A preliminary study of world weather. *Mem India Meteorol Dept* 4:53–84
- Wang B, Kang I-S, Lee J-Y (2004) Ensemble simulations of Asian–Australian monsoon variability by 11 AGCMs. *J Clim* 17:803–818
- Wang B, Lee J-Y et al (2009) Advance and prospect of seasonal prediction: assessment of the APCC/ClipAS 14-model ensemble retrospective seasonal prediction (1980–2004). *Clim Dyn* 33:93–117. doi:10.1007/s00382-008-0460-0
- Webster PJ, Houze RA Jr (1991) The equatorial mesoscale experiment, EMEX. *Bull Amer Meteor Soc* 72:1481–1505

- Webster PJ, Lukas R (1992) TOGA-COARE: The Coupled Ocean-Atmosphere Response Experiment. *Bull Amer Meteor Soc* 73:1377–1416
- Webster PJ, Magana VO, Palmer TN, Shukla J, Tomas RT, Yanai M, Yasunari T (1998) Monsoons: processes, predictability and the prospects of prediction. *J Geophys Res* 103:451–510
- Wu R, Kirtman BP (2003) On the impacts of Indian summer monsoon on ENSO in a coupled GCM. *Q J R Meteorol Soc* 129:3439–3468
- Xavier PK, Marzin C, Goswami BN (2007) An objective definition of the Indian summer monsoon season and a new perspective on the ENSO-monsoon relationship. *QJRM* 133:749–764
- Zhao M, Hendon HH (2009) Representation and prediction for the Indian Ocean dipole in the POAMA seasonal forecast model. *Q J R Meteorol Soc* 135:337–352